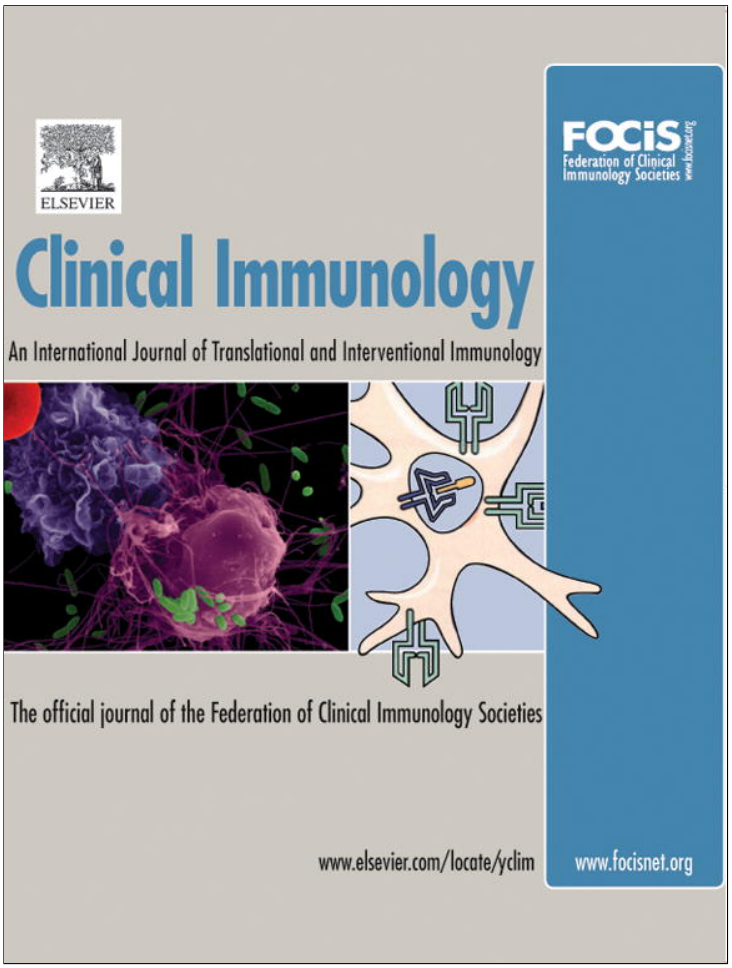

Clinical Immunology 161 (2015) 355–365

Contents lists available at ScienceDirect

Clinical Immunology

journal homepage: www.elsevier.com/locate/yclim

Lack of IL7Rα expression in T cells is a hallmark of T-cell immunodeficiency in Schimke immuno-osseous dysplasia (SIOD)

Mrinmoy Sanyal [a,b,*,1], Marie Morimoto [c,1], Alireza Baradaran-Heravi [d,1], Kunho Choi [c,1], Neeraja Kambham [b], Kent Jensen [e], Suparna Dutt [e], Kira Y. Dionis-Petersen [f], Lan Xiang Liu [f], Katie Felix [g], Christy Mayfield [h], Benjamin Dekel [i], Arend Bokenkamp [j], Helen Fryssira [k], Encarna Guillen-Navarro [l], Giuliana Lama [m], Milena Brugnara [n], Thomas Lücke [o], Ann Haskins Olney [p], Tracy E. Hunley [q], Ayse Ipek Polat [r], Uluc Yis [r], Radovan Bogdanovic [s], Katarina Mitrovic [s], Susan Berry [t], Lydia Najera [t], Behzad Najafian [u], Mattia Gentile [v], C. Nur Semerci [w], Michel Tsimaratos [x], David B. Lewis [f], Cornelius F. Boerkoel [c,**]

[a] Department of Medicine, Stanford University School of Medicine, Stanford, CA, USA
[b] Department of Pathology, Stanford University School of Medicine, Stanford, CA, USA
[c] Department of Medical Genetics and Child and Family Research Institute, University of British Columbia, Vancouver, BC, Canada
[d] Department of Biochemistry and Molecular Biology, University of British Columbia, Vancouver, BC, Canada
[e] Department of Medicine, Division of Rheumatology and Immunology, Stanford University School of Medicine, Stanford, CA, USA
[f] Department of Pediatrics, Division of Allergy, Immunology, and Rheumatology, Stanford University School of Medicine, Stanford, CA, USA
[g] Department of Cardiothoracic Surgery, Division of Pediatric Cardiothoracic Surgery, Lucile Packard Children's Hospital at Stanford, Stanford, CA, USA
[h] Warren Clinic, Tulsa, OK, USA
[i] Pediatric Stem Cell Research Institute, Safra Children's Hospital, Sheba Medical Center, Sackler School of Medicine, Tel Aviv, Israel
[j] Department of Pediatric Nephrology, VU University Medical Center, Amsterdam, The Netherlands
[k] Department of Medical Genetics, "Aghia Sophia" Children's Hospital, Athens University Medical School, Athens, Greece
[l] Sección de Genética Médica, Servicio de Pediatría, Hospital Clínico Universitario Virgen de la Arrixaca, IMIB-Arrixaca, Murcia, Spain; UCAM-Universidad Católica de Murcia, Spain; CIBERER-ISCIII, Madrid, Spain
[m] Department of Pediatrics, University of Naples, Naples, Italy
[n] Department of Pediatrics, University of Verona, Verona, Italy
[o] Department of Neuropediatrics, Children's Hospital, Ruhr-University Bochum, Bochum, Germany
[p] Department of Pediatrics, University of Nebraska Medical Center, Omaha, NE, USA
[q] Division of Pediatric Nephrology, Vanderbilt Children's Hospital, Nashville, TN, USA
[r] Department of Pediatrics, Dokuz Eylul University, Izmir, Turkey
[s] Institute of Mother and Child Health Care of Serbia and Faculty of Medicine, University of Belgrade, Belgrade, Serbia
[t] Department of Pediatrics, University of Minnesota Health System, Minneapolis, MN, USA
[u] Department of Pathology, University of Washington, Seattle, WA, USA
[v] Department of Medical Genetics, Hospital Di Venere – ASL Bari, Bari, Italy
[w] Department of Medical Genetics, School of Medicine, Pamukkale University, Denizli, Turkey
[x] Pediatric Multidisciplinary Unit, AP-HM Timone Enfant, Aix-Marseille University, Marseille, France

ARTICLE INFO

Article history:
Received 3 April 2015
Received in revised form 16 October 2015
accepted with revision 18 October 2015
Available online 21 October 2015

Keywords:
SIOD
T-cell immunodeficiency
IL7Rα

ABSTRACT

Schimke immuno-osseous dysplasia (SIOD) is an autosomal recessive, fatal childhood disorder associated with skeletal dysplasia, renal dysfunction, and T-cell immunodeficiency. This disease is linked to biallelic loss-of-function mutations of the *SMARCAL1* gene. Although recurrent infection, due to T-cell deficiency, is a leading cause of morbidity and mortality, the etiology of the T-cell immunodeficiency is unclear. Here, we demonstrate that the T cells of SIOD patients have undetectable levels of protein and mRNA for the IL-7 receptor alpha chain (IL7Rα) and are unresponsive to stimulation with IL-7, indicating a loss of functional receptor. No pathogenic mutations were detected in the exons of *IL7R* in these patients; however, CpG sites in the *IL7R* promoter were hypermethylated in SIOD T cells. We propose therefore that the lack of IL7Rα expression, associated with

Abbreviations: SIOD, Schimke immuno-osseous dysplasia; IL7Rα, interleukin-7 receptor alpha chain; PHA, phytohemagglutinin; PBMC, peripheral blood mononuclear cells.

* Correspondence to: M. Sanyal, Department of Medicine, Stanford University, VAPAHCS, Building 101, Room C4-171, 3801 Miranda Avenue, Palo Alto, CA, United States.
** Correspondence to: C.F. Boerkoel, Department of Medical Genetics, University of British Columbia, Children's and Women's Health Centre of British Columbia, 4500 Oak Street, Room C234, Vancouver, BC V6H 3N1, Canada.
E-mail addresses: msanyal@stanford.edu (M. Sanyal), boerkoel@interchange.ubc.ca (C.F. Boerkoel).
[1] These authors contributed equally in this study.

http://dx.doi.org/10.1016/j.clim.2015.10.005

CD127
CpG
Promoter DNA methylation

hypermethylation of the *IL7R* promoter, in T cells and possibly their earlier progenitors, restricts T-cell development in SIOD patients.

1. Introduction

Schimke immuno-osseous dysplasia (SIOD) is an autosomal recessive multi-system disorder. Prominent features of the disease are skeletal (spondyloepiphyseal) dysplasia, progressive renal failure with nephrotic proteinuria, and defective T-cell immunity [1–4]. Other less common features include hypothyroidism, abnormal dentition, bone marrow failure, thin hair, corneal opacities, atherosclerosis, stroke, and migraine-like headaches [2,4–8]. The SIOD expressivity ranges from in utero onset with growth retardation and death within the first 5 years of life to the onset of symptoms in late childhood [5,9,10].

Biallelic mutations of *SMARCAL1* have been associated with SIOD [11]. The *SMARCAL1* gene encodes a DNA annealing helicase with homology to the Switching defective 2 (SWI2) or Sucrose Non-Fermenting 2 (SNF2) (SWI2/SNF2) family of ATP-dependent chromatin remodeling proteins [12–15]. SMARCAL1 is a DNA stress response protein and participates in the maintenance of genomic integrity at stalled replication forks as well as in recombination, and gene expression [15–20].

Generally, SIOD-associated *SMARCAL1* nonsense and frameshift mutations lead to the loss of *SMARCAL1* mRNA. SIOD-associated *SMARCAL1* missense mutations impair SMARCAL1 sub-cellular localization, protein stability, ATPase activity, or chromatin binding [21]. The disease severity is inversely proportional to the overall SMARCAL1 activity [21]. Although, SMARCAL1 maintains genomic integrity and is involved in basic cellular functions including DNA repair, replication, recombination, and gene expression, it is still not clear why its deficiency results in the highly specific features of skeletal dysplasia, renal dysfunction, and T-cell lymphopenia.

We have shown that disease manifests when *SMARCAL1* deficiency interacts with genetic and environmental factors that further alter gene expression [17]. These alterations in gene expression, which are normally buffered by SMARCAL1, contribute to the penetrance of SIOD.

Here we report that T cells in SIOD patients are deficient in the expression of the IL-7 receptor alpha chain (IL7Rα or CD127) and are not responsive to stimulation with IL-7, indicating a loss of functional receptor. This possibly suggests a disruption of intrathymic T-cell development among SIOD patients. As a potential cause for the reduced IL7Rα expression, we detected hypermethylation of *IL7R* promoter CpG sites in T cells from SIOD patients.

2. Patients, materials, and methods

2.1. Subjects and families

SIOD patients (Table 1) referred to this study gave informed consent approved by the Institutional Review Board of Stanford University School of Medicine (Protocol ID: 419 and 27,191, Stanford, CA, USA) or of the University of British Columbia (H06-70283, Vancouver, BC, Canada). The protocol and informed consent procedures were provided according to the Declaration of Helsinki guidelines. The clinical data for patients were obtained from questionnaires completed by the attending physician as well as from the medical records. Cord blood samples were purchased from AllCells (Alameda, CA, USA).

2.2. Antibodies

Fluorescent-conjugated monoclonal antibodies against human CD3, CD4, CD8, CD45RA, CD45RO, CD25, CD127, and CD19 and isotype controls were purchased from BD Biosciences (San Diego, CA, USA). Anti-human CD31 antibody was purchased from BioLegend (San Diego, CA, USA). The complete list of antibodies used for flow cytometry is presented in Supplemental Table S1.

2.3. High-dimensional (Hi-D) (11-color) flow cytometry

Peripheral blood mononuclear cells (PBMC) from SIOD patients, unaffected siblings, and their parents, and normal controls were isolated by Ficoll–Hypaque density gradient centrifugation. Cells were then washed twice with Hank's balanced salt solution (HBSS) and either used immediately or frozen in fetal calf serum (FCS) containing 10% dimethyl sulfoxide (DMSO) until use. Single cell suspensions obtained

Table 1
SIOD patients analyzed in this study.

Patient ID	Genotype	Type of mutation	Effect	Age[a] (years)
SD18c	c.[1756C > T];[1756C > T]	Missense	p.[(R586W)];[(R586W)]	33
SD51	c.[2459G > A];[2542G > T]	Missense/nonsense	p.[(R820H)];[(E848X)]	17
SD60	c.[2542G > T];[2542G > T]	Nonsense	p.[(E848X)];[(E848X)]	12
SD74[b]	c.[1736C > T];[?]	Missense	p.[(S579L)];[(?)]	10
SD82	c.[1931G > A];[?]	Missense	p.[(R644Q)];[(?)]	21
SD100	c.[836 T > C];[?]	Missense	p.[(F279S)];[(?)]	26
SD107	c.[2542G > T];[2542G > T]	Nonsense	p.[(E848X)];[(E848X)]	3
SD108a	c.[1681C > T];[1681C > T]	Missense	p.[(R561C)];[(R561C)]	21
SD108b	c.[1681C > T];[1681C > T]	Missense	p.[(R561C)];[(R561C)]	7
SD112b	c.[1934G > A];[2542G > T]	Missense/nonsense	p.[(R645H)];[(E848X)]	19
SD119	c.[2449C > T];[2542G > T]	Missense/nonsense	p.[(R817C)];[(E848X)]	12
SD120	c.[2291G > A];[2542G > T]	Missense/nonsense	p.[(R764Q)];[(E848X)]	6
SD124	c.[1920_1921insG];[1920_1921insG]	Nonsense	p.[(V641fsX51)];[(V641fsX51)]	7
SD131	c.[1026C > A];[2264 T > G]	Missense/nonsense	p.[(Y342X)];[(I755S)]	4
SD136a	c.[863-2A > G];[863-2A > G]	Splice site	p.[(M288_D366del)];[(M288_D366del)]	9
SD136b	c.[863-2A > G];[8632A > G]	Splice site	p.[(M288_D366del)];[(M288_D366del)]	8
SD138	c.[2542G > T];[2542G > T]	Nonsense	p.[(E848X)];[(E848X)]	4
SD139	c.[1190delT];[2575 T > C]	Nonsense/missense	p.[(L397fsX40)];[(S859P]	8
SD146	c.[1642_1644delATT];[1642_1644delATT]	In frame deletion	p.[(I548del)];[I548del)]	3
SD148	c.[740G > C];[2542G > T]	Missense/nonsense	p.[(R247P)];[(E848X)]	8
SD150	c.[2459G > A];[2459G > A]	Missense	p.[(R820H)];[R820H)]	4

[a] Age at sample collection.
[b] Although only one *SMARCAL1* mutation was detected in this patient, we previously showed that the other allele did not express *SMARCAL1* mRNA [37].

from fresh preparation or from frozen aliquots were stained with a combination of fluorochrome-conjugated antibodies against CD3, CD4, CD8, CD45RA, CD45RO, CD25, CD127, CD19, CD31, and isotype controls (BD Biosciences, San Diego, CA, USA). "Fluorescence-minus-one" controls were included to determine the level of nonspecific staining and autofluorescence associated with subsets of cells in each fluorescence channel. For surface staining, propidium iodide was added to all of the samples before data collection to identify dead cells. Hi-dimensional flow cytometry data were collected on a LSRII FACS instrument (BD Biosciences, San Jose, CA, USA). FlowJo (TreeStar, San Carlos, CA, USA) software was used for fluorescence compensation and analysis. Data are depicted as contour plots, or histograms displaying fluorescence intensity (FI) plotted against cell numbers/FI interval with a total of 256 intervals per parameter.

Spleen samples were washed twice with phosphate buffered saline (PBS), then once with RPMI 1640 media containing 10% FCS. Single cell suspensions were prepared by passing the tissue through a 70-μm nylon mesh and collected in PBS. Mononuclear cells from the single cell suspension were isolated by Ficoll–Hypaque density gradient centrifugation. Cells were then washed and either used immediately or frozen in FCS containing 10% DMSO until use. Cells were stained as described above.

2.4. Immunohistochemistry

A fresh spleen sample from an SIOD patient was obtained after autopsy. Portions of the tissue were formalin-fixed and paraffin-embedded (FFPE) using standard procedures. FFPE normal spleen samples were obtained from the archives of the Department of Pathology, Stanford University Medical Center (Stanford, CA) following Institutional Review Board approval. Four μM-thick sections from paraffin-embedded tissue blocks were de-paraffinized in xylene and hydrated in a series of graded alcohols. Heat-induced antigen retrieval was carried out by microwave pretreatment in citric acid buffer (10 mM citric acid, pH 6.0) for 10 min. Sections were stained with an anti-human CD3 antibody (clone UCHT1) at a dilution of 1:100. Detection was carried out using the DAKO Envision method (DAKO Corporation, Carpinteria, CA, USA). Additional sections were stained with hematoxylin and eosin (H&E).

2.5. Lymphocyte proliferation assays

PBMCs were incubated with 1 μM carboxyfluorescein succinimidyl ester (CFSE) (Invitrogen, Carlsbad, CA, USA) for 7 min in serum-free media at room temperature. Cells were then washed twice with RPMI 1640 media containing 10% FCS. CFSE-labeled cells were plated in round-bottom 96 well plates at a density of 5×10^5 cells/well. Some wells were incubated with 100 ng/ml recombinant human IL-7 (R&D Systems, Minneapolis, MN, USA). For the induction of proliferation, cells were incubated with anti-CD3/CD28 conjugated beads (Invitrogen, Carlsbad, CA, USA) at a bead to cell ratio of 1:100. Control cells were left unstimulated. After incubation for 96 h, cells were washed once with PBS, stained with antibodies against CD3, CD4, and CD8 and washed again. Propidium iodide was added to each sample to identify dead cells and analyzed by flow cytometry. Cell divisions were quantified by the loss of CFSE fluorescence using FlowJo software.

2.6. RNA isolation and reverse transcription

RNA from purified T cells or PBMCs was extracted using the RNeasy Mini Kit (Qiagen, Toronto, ON, Canada), and on-column DNase I digestion (Qiagen, Toronto, ON, Canada) was performed to remove genomic DNA. Reverse transcription was performed with the qScript™ cDNA Synthesis Kit (Quanta Biosciences, Gaithersburg, MD, USA) according to the manufacturer's specifications.

2.7. Quantitative PCR

SsoFast EvaGreen Supermix (Bio-Rad Laboratories, Mississauga, ON, Canada) was used with the ABI 7500 Fast Real-Time PCR System for quantitative PCR. The following conditions were used for amplification: 1 cycle of 95 °C for 30 s, followed by 40 cycles of 95 °C for 5 s, and 60 °C for 30 s, followed by a melt curve analysis.

The relative quantification of gene expression was calculated using the ΔΔCt method [22]. Expression of the housekeeping gene *GAPDH* was used as the internal control. Graphed quantitative data are presented as the mean ± standard deviation calculated from three technical replicates. The primer sequences used in this study are listed in Supplemental Table S2.

2.8. Sequencing of SMARCAL1 cDNA

For those SIOD patients for whom we only detected one heterozygous *SMARCAL1* mutation, we synthesized cDNA from patient PBMC RNA and sequenced the coding region of the *SMARCAL1* cDNA following PCR amplification. The amplified fragments were sequenced by the Sanger method (Macrogen, Seoul, Korea), and the sequences were aligned and analyzed using Sequencher v.4.10.1 (Gene Codes, Ann Arbor, MI, USA). The sequences of all of the primer pairs used for PCR amplification and sequencing are presented in Supplemental Table S3.

2.9. Sequencing of IL7R exons

To determine whether SIOD patients have mutations in the *IL7R* gene, all coding exons of the gene were amplified by PCR and sequenced. DNA was extracted from peripheral whole blood using the Gentra Puregene Blood Kit (Qiagen, Toronto, ON, Canada) according to the manufacturer's protocol. The amplified fragments were sequenced by the Sanger method (Macrogen, Seoul, Korea), and the sequences were aligned and analyzed using Sequencher v.4.10.1 (Gene Codes, Ann Arbor, MI, USA). The sequences of all of the primer pairs used for PCR and sequencing are presented in Supplemental Table S4.

2.10. Bisulfite pyrosequencing

$CD3^+$ T cells were FACS purified from the peripheral blood of 7 SIOD patients and their age- and sex-matched controls. The average DNA methylation of 6 CpG sites in the *IL7R* promoter was analyzed by bisulfite pyrosequencing as previously described [23]. For each sample, genomic DNA of 2×10^4–1×10^5 $CD3^+$ T cells was bisulfite converted using the EZ DNA Methylation-Direct Kit (Zymo Research, Irvine, CA, USA) according to the manufacturer's instructions. The efficiency of bisulfite treatment, measured by the conversion of cytosines not followed by guanosines into uracils, was >97% in all experiments. The regions of interest in the *IL7R* promoter were then PCR amplified and subsequently sequenced using the PyroMark Gold Q96 Reagents (Qiagen, Toronto, ON, Canada) and the PyroMark Q96 MD system (Qiagen, Toronto, ON, Canada). The forward, reverse, and sequencing primers and PCR conditions have been previously described [23] and are listed in Supplemental Table S5. The average DNA methylation for each CpG site in the *IL7R* promoter at positions −1064, −656, −586, −563, −555, and −435 relative to the translation start site was evaluated using the PyroMark CpG software (Qiagen, Toronto, ON, Canada). Human High and Low Methylated Genomic DNA (EpigenDx, Hopkinton, MA, USA) were respectively used as positive and negative DNA methylation controls for the bisulfite pyrosequencing assays.

2.11. Measurement of serum immunoglobulin isotypes and IgG subtypes

Serum immunoglobulin isotypes and IgG subtypes concentrations were measured using MILLIPLEX X-MAP Human Isotyping Kit (HGAMMAG-301 K, Millipore, Billerica, MA) that utilizes magnetic

microsphere-conjugated capture antibodies. The manufacturer has validated the panel for serum immunoglobulin measurement. Archived serum samples from SIOD patients and controls were diluted 1:16,000 using dilution buffer according to the manufacturer's protocol. Fluorescent intensities of the microspheres with captured antibodies were analyzed and the final concentrations were calculated using Bio-Plex 200 System (Bio-Rad, Hercules, CA). Serum concentration of total IgG was measured using the Human Immunoglobulin G ELISA Kit (Molecular Innovations, Novi, MI) following the manufacturer's instructions.

2.12. Statistical analyses

p values were determined by the two-tailed Student's *t*-test for independent samples assuming equal variances on all experimental data

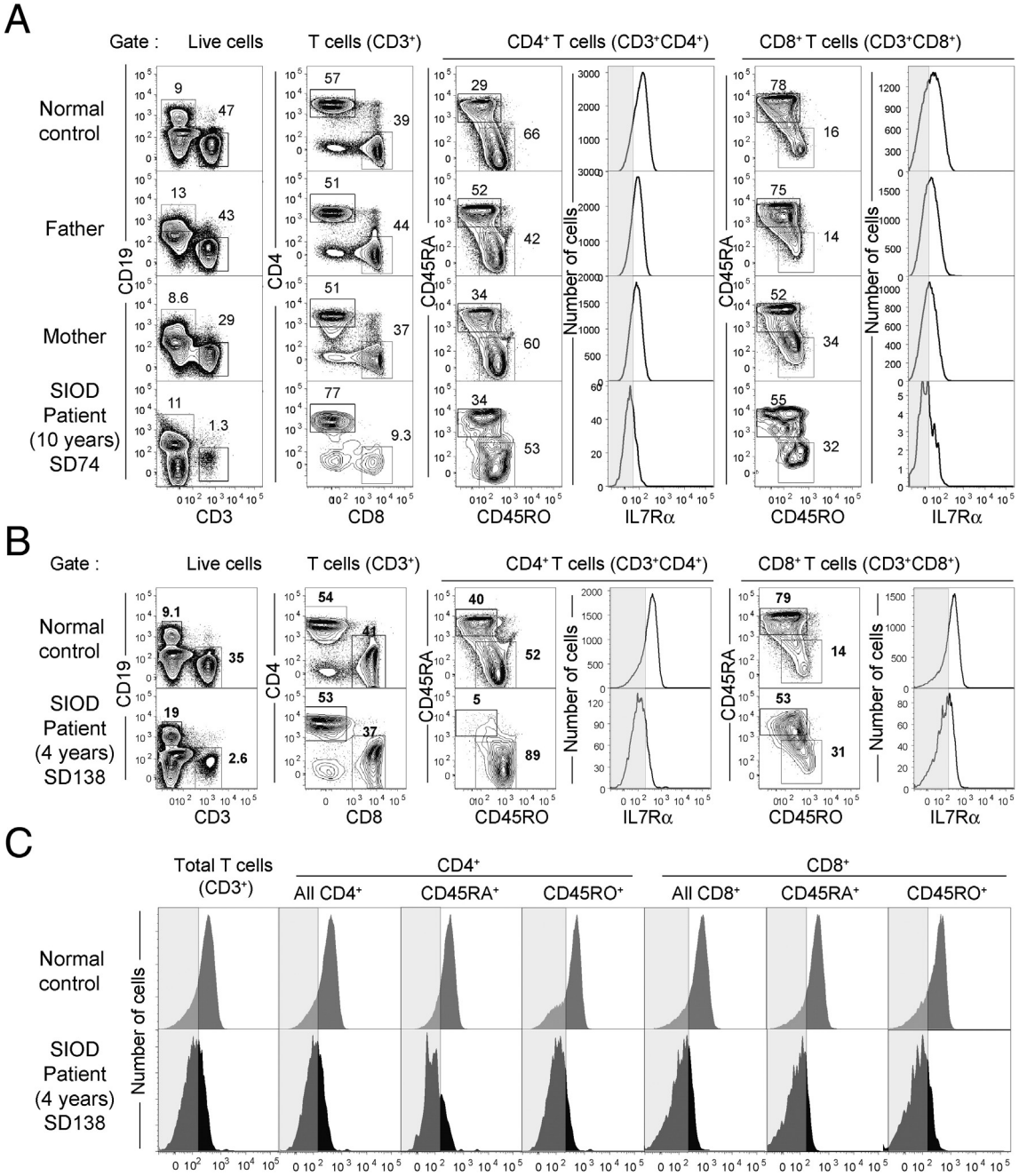

Fig. 1. Phenotypic analyses of T cells from SIOD patients reveal high proportions of memory T cells and deficiency of IL7Rα expression. (A and B) Peripheral blood mononuclear cells (PBMC) from SIOD patients, parents and normal controls were stained with fluorescent-conjugated anti-human CD19, CD3, CD4, CD8, CD45RA, CD45RO and CD127 (IL7Rα) antibodies. Initially, B and T cells were identified based on CD19 and CD3 expression (left column panel). T cells ($CD3^+$) were subsequently resolved for CD4 and CD8 subsets (middle column panels). Both of these subsets were further resolved for naïve ($CD45RA^+CD45RO^-$) and memory ($CD45RA^-CD45RO^+$) T cells (middle right and right panels, respectively). Expression of IL7Rα in $CD4^+$ and $CD8^+$ is presented as histograms. Shaded regions in the histogram plots represent signals from isotype control staining. Note that SIOD patients SD74 (panel A) and SD138 (panel B) have reduced IL7Rα expression that overlaps with isotype control staining. These are representative data. (C) Expression of IL7Rα (CD127) from gated T-cell subsets from the SIOD patient and normal control presented in B is shown here. Shaded regions in the histogram plots represent signals from isotype control staining. Note that total $CD4^+$, naïve $CD4^+$ cells ($CD4^+$ $CD45RA^+CD45RO^-$), memory $CD4^+$ cells ($CD4^+CD45RA^-CD45RO^+$), total $CD8^+$, naïve $CD8^+$ cells ($CD8^+CD45RA^+CD45RO^-$) and memory $CD8^+$ cells ($CD8^+$-$CD45RA^-CD45RO^+$) uniformly express reduced IL7Rα in SIOD patients. These are representative data.

sets. For the analysis of the average DNA methylation of *IL7R* promoter CpG sites, the one-tailed Mann–Whitney U Test was performed.

3. Results

3.1. SIOD patients are T-cell lymphopenic and are deficient in IL-7 receptor alpha chain (CD127)

SIOD patients are T-cell lymphopenic [5]. However, T-cell subset distribution in these patients has not been analyzed in detail. Initially, we resolved different lymphocyte subsets in the SIOD patients by hi-dimensional flow cytometry (Fig. 1A). B and T cells were identified based on CD19 and CD3 expression, respectively. T cells ($CD3^+$) were subsequently resolved for $CD4^+$ and $CD8^+$ subsets. Based on CD45RA and CD45RO expression, $CD3^+CD4^+CD8^-$ and $CD3^+CD4^-CD8^+$ T cells were further resolved into naïve ($CD45RA^+CD45RO^-$) or memory ($CD45RA^-CD45RO^+$) T-cell subsets. We then analyzed the expression of the IL7Rα chain (CD127) in the T cells of SIOD patients and unaffected individuals (Fig. 1).

As previously reported [5], we observed that SIOD patients are T-cell lymphopenic compared to normal individuals (Fig. 1A and B). In the T-cell compartments, their CD4 to CD8 ratios were usually normal (8 out of 10 patients analyzed). From an early age, SIOD patients had very high proportions of memory cells ($CD45RA^-CD45RO^+$) compared to naïve cells ($CD45RA^+CD45RO^-$) in both $CD4^+$ and $CD8^+$ subsets (9 out of 10 patients analyzed). IL7Rα expression was nearly undetectable in the T cells from SIOD patients (21 out of 21 patients analyzed) (Figs. 1A and B, 2 and Supplemental Fig. S3). The fluorescent signals for patient T cells nearly overlapped with the signal from isotype control staining suggesting a complete lack of IL7Rα expression.

3.2. Reduction of IL7Rα is not restricted to any specific T-cell subset

To address whether the reduction of IL7Rα expression was restricted to a particular subset of T cells, we analyzed its expression in gated T-cell subsets (Fig. 1C) including total, naïve ($CD45RA^+CD45RO^-$) and memory ($CD45RA^-CD45RO^+$) subsets of $CD4^+$ and $CD8^+$ T cells. Our analysis revealed that all of the subsets have uniformly reduced IL7Rα

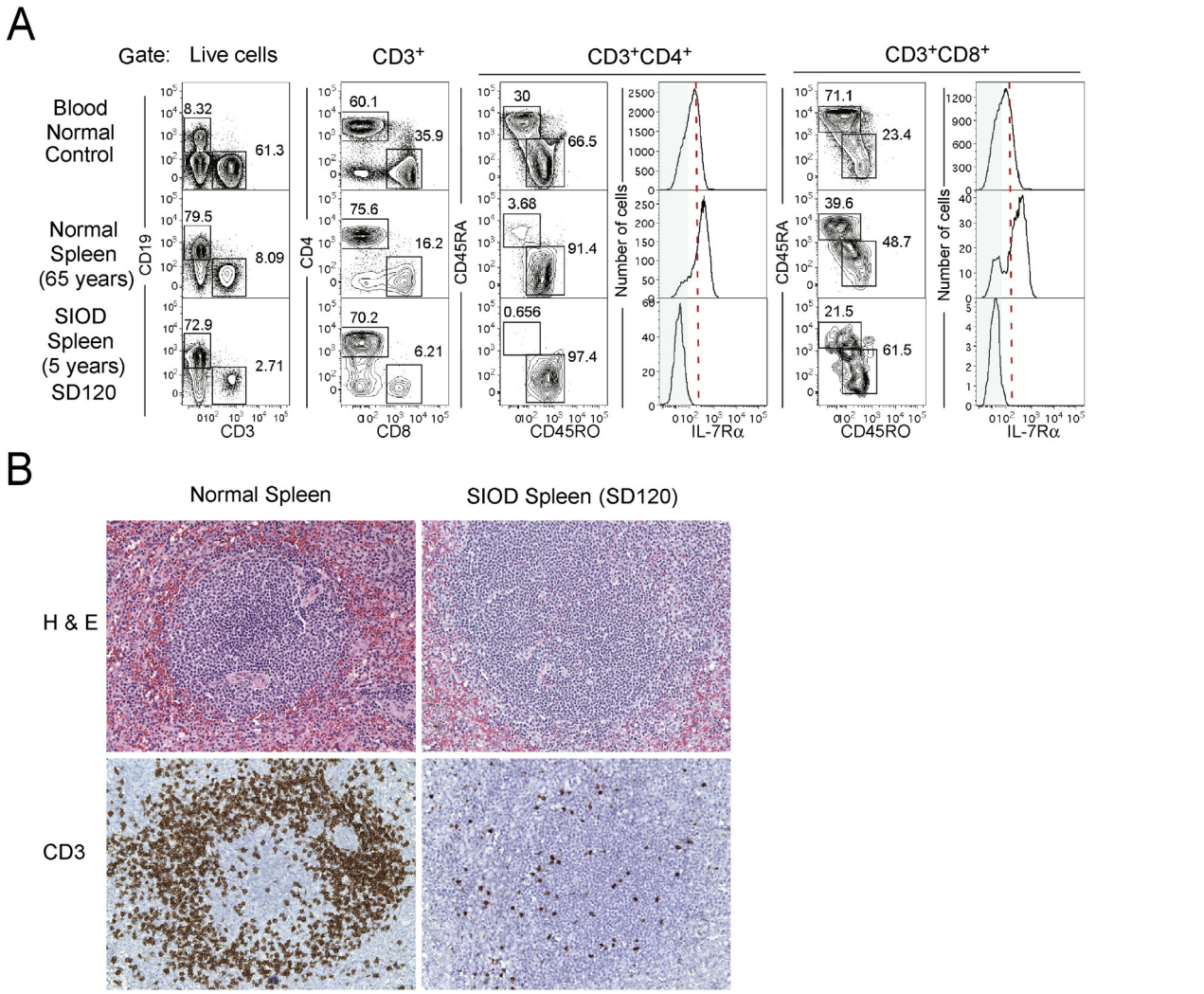

Fig. 2. An SIOD spleen has very few T cells and reduced IL7Rα expression. (A) Mononuclear cells prepared from normal and SIOD spleens were analyzed for different T-cell subsets as in Fig. 1. Similar to the peripheral blood of SIOD patients (Fig. 1), analysis of splenic tissue from a 5-year-old patient (SD120) showed very few $CD3^+$ T cells. Although, it seems that the CD4 verses CD8 T-cell ratio is affected in this SIOD spleen, subset analysis of these T cells revealed that they mostly display a memory phenotype in both CD4 and CD8 compartments ($CD45RA^-CD45RO^+$). Expression of IL7Rα in T cells was severely reduced in the SIOD spleen compared to a normal spleen from a 65-year-old donor with a similar memory to naïve cell subset distribution as observed in the SIOD spleen. (B) Histopathological analysis revealed that the SIOD spleen (400×) was nearly devoid of T cells in the lymphoid follicles and in the intra-follicular space. Upper panels show hematoxylin and eosin staining (H&E). Bottom panels show CD3 staining of formalin-fixed and paraffin-embedded sections.

expression indicating that the deficiency had likely arisen very early during intrathymic T-cell development (Fig. 1C).

3.3. SIOD splenic T cells also have reduced IL7Rα expression

The analysis of 21 patients and their family members revealed that SIOD patients have IL7Rα deficiency in their peripheral blood T cells and that those T cells mostly display a memory phenotype. Because this skewed representation of T cells in peripheral blood may have altered the expression of IL7Rα, we analyzed IL7Rα expression in splenic T cells from an SIOD patient (SD120) (Fig. 2). When compared with T cells from the spleen of an unaffected individual with a similar memory to naïve T-cell subset representation, we noticed a similar reduction of IL7Rα expression (Fig. 2A) as among the peripheral blood T cells. This demonstrates that altered subset distribution is not the primary cause of the reduced IL7Rα expression. Histopathological analysis showed normal tissue architecture in the SIOD spleen but very few T cells (Fig. 2B).

3.4. SIOD T cells have reduced IL7R mRNA levels

To address whether the reduction of surface expression of IL7Rα had arisen from altered mRNA synthesis, we purified T cells from a normal control subject and four SIOD patients (Fig. 3A) and measured relative *IL7R* mRNA levels. We observed that SIOD T cells had significantly reduced relative *IL7R* mRNA levels compared to a normal control (Fig. 3B). IL7Rα protein expression therefore correlates with transcript level, and we conclude that this likely arises from reduced *IL7R* expression.

3.5. T cells in SIOD patients are not responsive to IL-7

Interleukin-7 (IL-7), produced by stromal cells and thymic epithelial cells, is a ligand for IL7Rα. Signaling via the IL-7 and IL7Rα system is important for T-cell development, survival, and proliferation. Since SIOD T cells do not express IL7Rα, we verified functional loss of the receptor by measuring IL-7 induced enhancement of T-cell proliferation (Fig. 4 and Supplemental Fig. S2). To develop this assay, we stimulated normal PBMCs with increasing concentrations of recombinant IL-7 and analyzed the proliferation of $CD4^+$ and $CD8^+$ T cells. We found that IL-7 concentrations of 1 ng/ml to 1000 ng/ml alone did not induce proliferation or apoptosis of $CD4^+$ or $CD8^+$ T cells (Supplemental Fig. S1A); however, the combination of sub-optimal amounts of CD3/CD28 conjugated beads, which induce moderate T-cell proliferation (Supplemental Fig. S1B), with 100 ng/ml of IL-7 induced a marked proliferation of $CD4^+$ and $CD8^+$ cells (Supplemental Fig. S1B). Measuring IL-7 induced enhancement of proliferation in SIOD T cells (Fig. 4), we found that both SIOD $CD4^+$ (Fig. 4A) and $CD8^+$ (Fig. 4B) T cells failed to respond to IL-7, although when stimulated with optimum (1:1 cell to beads ratio) CD3/CD28 beads, they proliferated normally. Also, a normal response was noted when SIOD T cells were stimulated with phytohemagglutinin (PHA) or interleukin-2 (IL-2) (Supplemental Fig. S2). These observations suggest that the lack of response to IL-7 is specific and likely due to the deficiency of IL7Rα expression. We conclude therefore that there is a functional loss of the IL-7 receptor in SIOD T cells.

3.6. DNA changes in the IL7R gene in SIOD are not pathogenic

Mutations in *IL7R* have been reported to abolish the expression of IL7Rα leading to T-cell immunodeficiency [24,25]. To test this as a potential mechanism of IL7Rα deficiency in SIOD patients, we sequenced the coding regions (exons) of *IL7R* from three patients and their parents. Our sequencing results identified five common polymorphisms of *IL7R* in these SIOD patients (Table 2).

3.7. Reduced thymic output in SIOD patients

T-cell deficiency in SIOD patients could arise from defective thymic function leading to decreased thymic output or from peripheral T-cell loss. Thymic output is correlated with the abundance of recent thymic emigrant ($CD4^+CD45^+CD31^+$) cells in the peripheral blood [26]. To differentiate these two possibilities, we analyzed the frequency of $CD4^+CD45^+CD31^+$ cells in the peripheral blood of SIOD patients. Fig. 5 shows the progressive decrease of $CD4^+CD45^+CD31^+$ T cells in the peripheral blood with increasing age (cord blood, 19- and 45-year-old) among normal individuals. In contrast, the peripheral blood of SIOD patients was nearly devoid $CD4^+CD45^+CD31^+$ cells at any age. This observation suggests decreased thymic output among SIOD patients.

3.8. CpG sites in the IL7R promoter are hypermethylated in SIOD T cells

Methylation of CpG sites in the *IL7R* promoter diminishes the expression of IL7Rα in $CD8^+$ T cells [23]. To explore the possibility of promoter hypermethylation as a potential mechanism for the diminished expression of *IL7R* in SIOD patients, we sorted $CD3^+$ cells from a cohort of 7 SIOD patients along with age- and sex-matched controls and analyzed the average DNA methylation status of 6 CpG sites in the *IL7R* promoter by bisulfite pyrosequencing (Fig. 6A). We observed that the CpG sites most proximal to the translation start

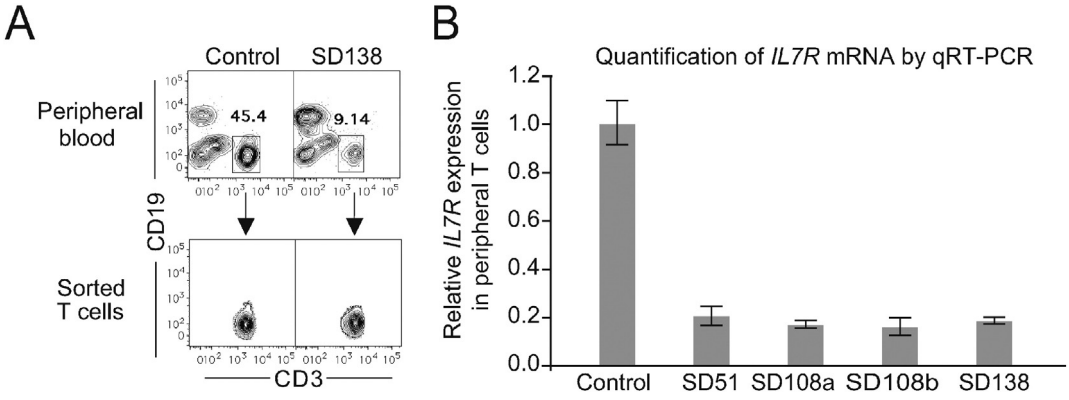

Fig. 3. *IL7R* mRNA expression is reduced in SIOD T cells. (A) The scheme for sorting T cells from peripheral blood. (B) Relative *IL7R* mRNA levels of peripheral blood $CD3^+$ T cells from a normal control and four SIOD patients (SD51, SD138, SD108a, SD108b) measured by qRT-PCR. The *IL7R* mRNA levels of three technical replicates were standardized to the mRNA levels of the housekeeping gene *GAPDH* and graphed relative to control. Error bars represent one standard deviation.

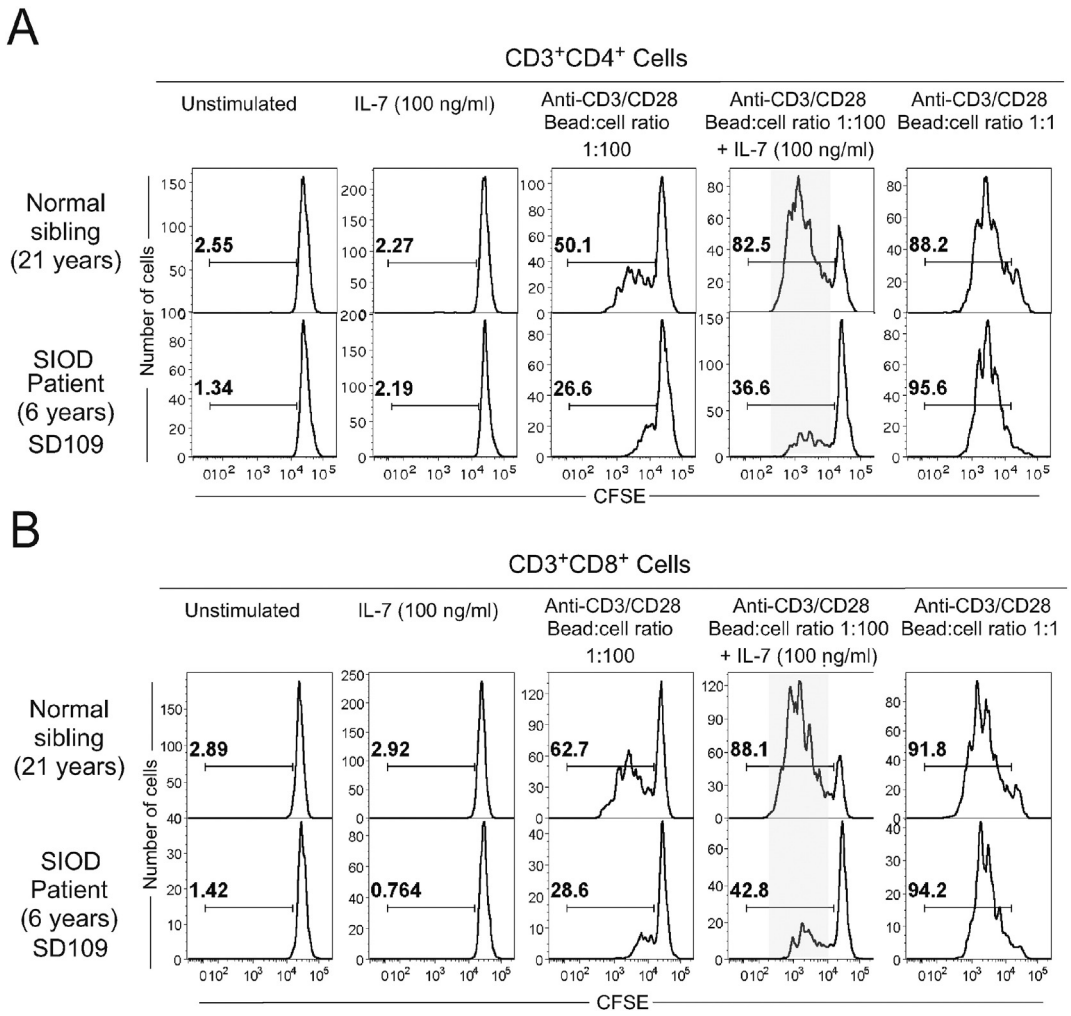

Fig. 4. T cells in SIOD patients fail to respond to IL-7. (A) PBMCs were labeled with CFSE, and cultured for 96 h. Anti-CD3/CD28 beads at a bead to cell ratio of 1:100 were used to induce T-cell proliferation. Cells were incubated with 100 ng/ml IL-7 to determine its effect on T cells with or without anti-CD3/CD28 beads. After incubation for 96 h, T-cell subsets were resolved using fluorochrome-conjugated anti-human CD3, CD4 and CD8 antibodies. Cellular proliferation was measured by CFSE dilution. Representative analyses from three SIOD patients and controls are shown. Note that the $CD4^+$ T cells from SIOD patients did not respond to IL-7 induced enhancement of T-cell proliferation. (B) Similar reduced IL-7 responsiveness was observed in SIOD $CD8^+$ T cells.

site (i.e., −656, −586, −563, −555, and −435) were significantly hypermethylated in SIOD patients (Fig. 6B), whereas the more distal CpG site (i.e., −1064) was comparably methylated to unaffected individuals.

4. Discussion

SIOD is a multi-system disorder predominantly involving the skeleton, kidney, and immune systems [1–5], although additional systems

Table 2
Exon sequencing results of *IL7R* in SIOD families.

Nucleotide change	Amino acid change	SNP	Proband genotype	Paternal genotype	Maternal genotype
Pedigree SD18					
c.82 + 16G > C	NA	rs1353252	Heterozygous	Homozygous	No Change
c.197 T > C	p.Ile66Thr	rs1494558	Heterozygous	Homozygous	No Change
c.412G > A	p.Val138Ile	rs1494555	Heterozygous	Homozygous	No Change
c.1066A > G	p.Ile356Val	rs3194051	Heterozygous	Heterozygous	No Change
Pedigree SD74					
c.82 + 16G > C	NA	rs1353252	Heterozygous	Heterozygous	Heterozygous
c.197 T > C	p.Ile66Thr	rs1494558	Heterozygous	Heterozygous	Heterozygous
c.412G > A	p.Val138Ile	rs1494555	Heterozygous	Heterozygous	Heterozygous
c.1066A > G	p.Ile356Val	rs3194051	Heterozygous	Heterozygous	No Change
Pedigree SD120					
c.82 + 16G > C	NA	rs1353252	Homozygous	Heterozygous	Homozygous
c.197 T > C	p.Ile66Thr	rs1494558	Homozygous	Heterozygous	Homozygous
c.412G > A	p.Val138Ile	rs1494555	Homozygous	Heterozygous	Homozygous
c.495C > T	p.His165His	rs2228141	Heterozygous	No Change	Heterozygous
c.1066A > G	p.Ile356Val	rs3194051	Heterozygous	Heterozygous	No Change

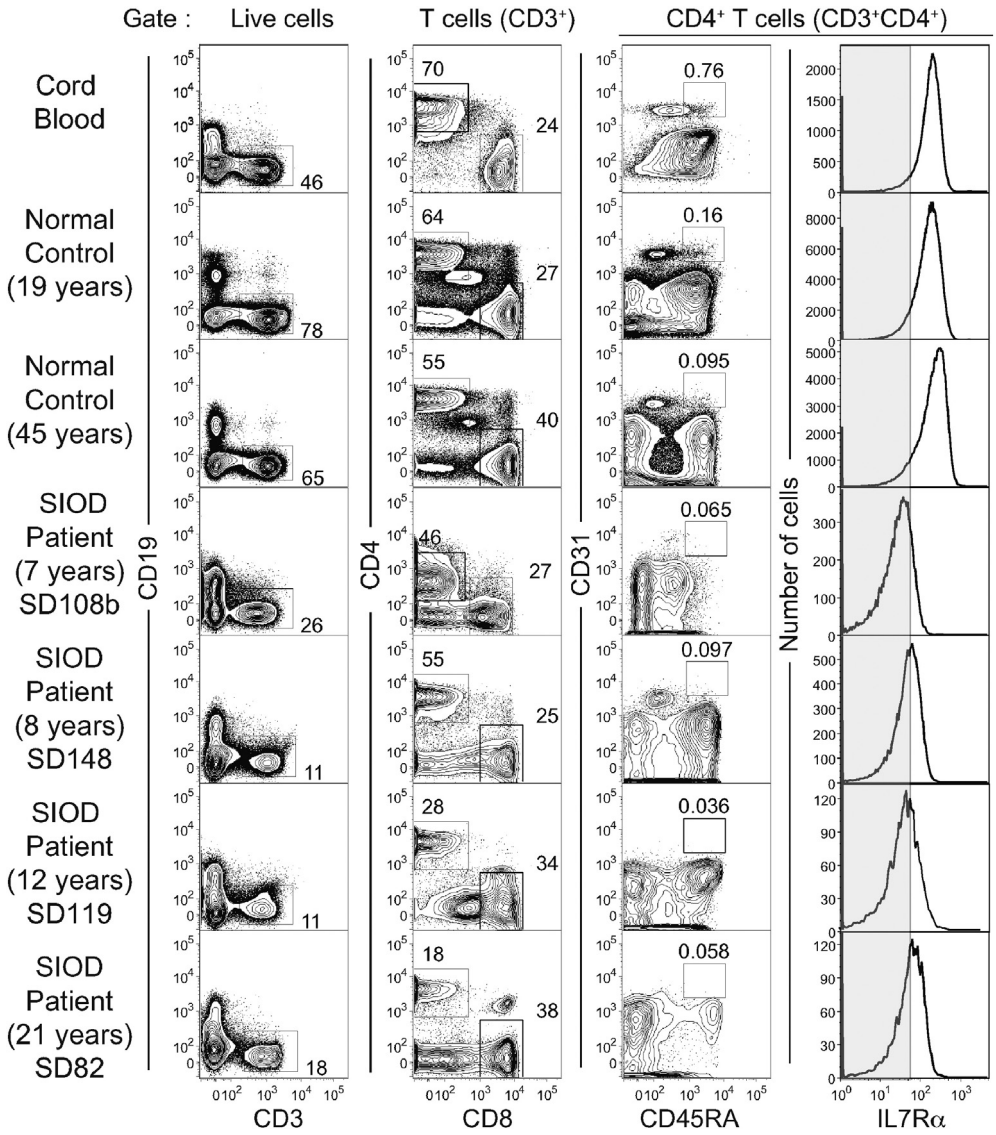

Fig. 5. Reduced thymic output in SIOD patients. Cord blood mononuclear cells and peripheral blood mononuclear cells (PBMC) from SIOD patients along with normal controls at different ages were stained with fluorescent-conjugated anti-human CD19, CD3, CD4, CD8, CD45RA, CD45RO, CD127 (IL7Rα) and CD31 antibodies. Initially, T cells were identified based on CD3 expression (left column panel). T cells ($CD3^+$) were subsequently resolved for CD4 and CD8 subsets (middle column panels). $CD3^+CD4^+$ subsets were further analyzed for CD45RA and CD31 expression (third column panels). Recent thymic emigrant cells corresponding to $CD4^+CD45RA^+CD31^+$ cells are marked by rectangular gates in the third column panels. Expression of IL7Rα in $CD3^+CD4^+$ cells are presented as histograms in the forth column panels. Shaded regions in the histogram plots represent signals from isotype control staining. Note that there is a progressive decrease of $CD4^+CD45RA^+CD31^+$ cells with age in the normal controls. Two cord blood samples and peripheral blood samples from normal individuals of ages 18, 19, 21, 25, 45 and 65 were analyzed; data from 1 cord blood sample and 3 peripheral blood samples of representative ages are shown here. Also note that the SIOD patients are nearly devoid of $CD4^+CD45RA^+CD31^+$ cells and have reduced IL7Rα expression that overlaps with isotype control staining. Peripheral blood samples from 6 SIOD patients were analyzed; data from 4 patient peripheral blood samples are shown here.

are often involved. Among the immune phenotypes, the most prominent is primary T-cell immunodeficiency [5,27]. Recurrent infection, due to T-cell deficiency accounts for significant mortality in SIOD patients. Herein we identify deficiency of IL7Rα expression as an etiology of this T-cell immunodeficiency.

Primary immunodeficiency diseases are a heterogeneous group of disorders resulting from intrinsic defects of the immune system [28]. They are frequently associated with repeated bacterial, fungal, or viral infections and cause significant morbidity and mortality [28]. In normal human T-cell development, T-lineage committed progenitors, arising from the bone marrow, home to the thymus and differentiate through successive stages of development to produce immature CD4 and CD8 T cells. These cells then leave the thymus and enter the periphery and further mature. Generation of T-cell clonal diversity also occurs within the thymus, and peripheral T cells in SIOD patients are mono- or oligoclonal [29] suggesting defective T-cell development.

The cytokine IL-7, produced by thymic stromal cells, is essential for T-cell development. Genetic ablation of the *Il7* gene in the mouse severely impairs T-cell (and B-cell) development [30,31]. This cytokine signals through the IL-7 receptor complex, which consists of the IL7Rα chain and the common gamma chain (γc) [32]. In humans, either complete [24] or partial [25] deficiency of IL7Rα abrogates T-cell development and causes severe T-cell deficiency. In mice, deletion of the *Il7r* gene that encodes for IL7Rα severely disrupts T-cell development and impairs B-cell development [33]. In contrast, oncogenic gain-of-function *IL7R* mutations lead to childhood T-cell acute lymphoblastic leukemia [34]. Thus, IL-7 and its receptor system (IL7R) play a critical and non-redundant role for early T-cell development and homeostasis. Any aberration in expression and function of these two molecules severely alters T-cell homeostasis. In this context, our observations suggest that the lack of IL7Rα expression is the likely cause of the T-cell immunodeficiency in SIOD patients.

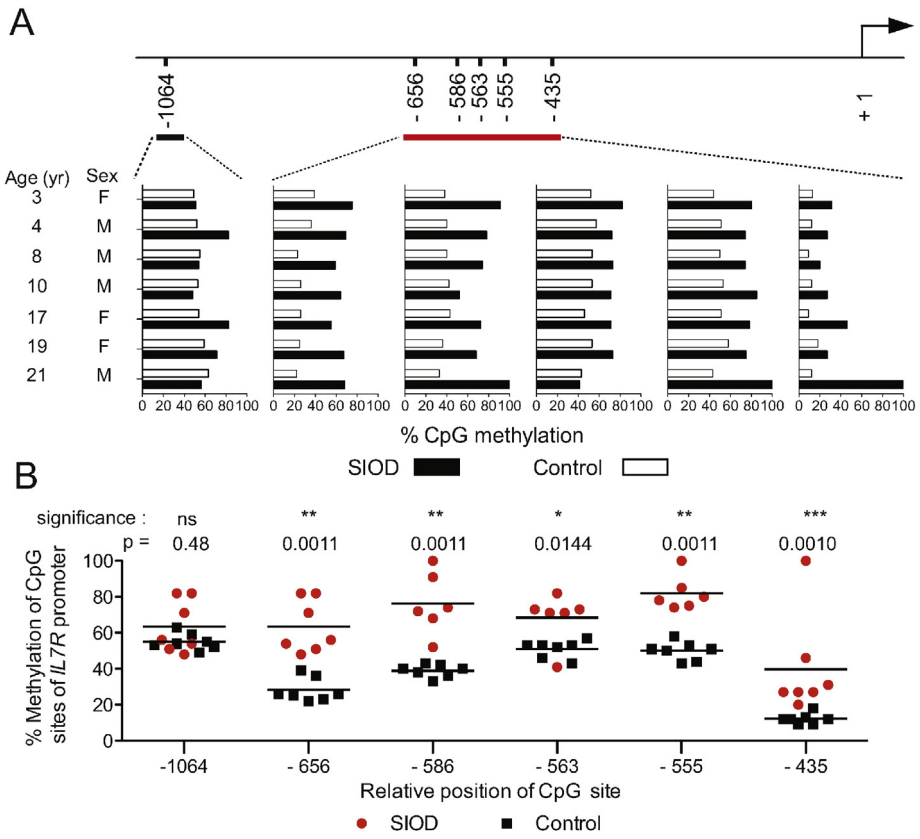

Fig. 6. *IL7R* promoter CpG sites are hypermethylated in SIOD patients. (A) $CD3^+$ T cells were sorted from 7 SIOD patients and their age- and sex-matched controls as in Fig. 2C. Genomic DNA isolated from the sorted cells was analyzed for the methylation status of six individual CpG sites in the *IL7R* promoter. The average percent methylation of all six CpG sites relative to the translational start site in the *IL7R* gene promoter for the patients and normal control subjects is shown. (B) Comparison of average percent methylation of each CpG site between SIOD patients and normal control subjects is shown. The median values for all SIOD patients and the normal control subjects for each site are indicated by a horizontal line. The one-tailed Mann–Whitney U Test was used to compare the values for each site between the SIOD patients and the normal controls. The calculated *p* values for each of the sites are indicated above the respective site; a *p* value of less than 0.05 was considered to be statistically significant. Note that, except for the CpG at position −1064, all other sites are significantly hypermethylated. ns, not significant; *, $p < 0.05$; **, $p < 0.01$; ***, $p < 0.001$.

Functional IL-7 receptor is composed of two chains, the alpha chain (IL7Rα) and the common gamma chain (γc) shared by several other cytokine receptors (IL-2, −9, −15 and −21). Among γc expressing receptors, the IL-2 receptor is abundantly expressed in T cells. Our demonstration that SIOD T cells do not respond to IL-7 stimulation (Fig. 4) but respond normally to IL-2 (Fig. S2) confirms that the γ chain is functional, whereas the α chain of IL7Rα is not functional. We have shown that all subsets of T cells in SIOD patients lack IL7Rα expression including naïve T cells ($CD45RA^+CD45RO^-$) (Fig. 1B). This suggests that the defect in IL7Rα expression in T cells may have arisen intrathymically, i.e., before the cells reached the periphery.

Although the T-cell deficiency in SIOD patients could be the result of defective thymic output or peripheral T-cell loss, our demonstration that SIOD patients are devoid of $CD4^+CD45^+CD31^+$ recent thymic emigrant cells (Fig. 5), and the overall decrease of naïve T cells ($CD45RA^+$-$CD45RO^-$) in both CD4 and CD8 compartments from an early age indicates that defective thymic output is the likely cause of the T-cell deficiency in SIOD patients. Additionally, the normal proliferative response of SIOD T cells upon stimulation with optimum anti-CD3/CD28 antibodies (Fig. 4) and mitogen (PHA) (Supplemental Fig. S2) in presence of IL-2 suggest that the lack of peripheral proliferation or decreased survival after migration of T cells to the periphery are unlikely to be causes of the T-cell deficiency.

We anticipated that although SIOD patients have normal numbers of B cells, they would have impaired B-cell function, particularly functions requiring T-cell help, because their very few T cells are predominantly memory T cells. To understand this, we quantified serum concentrations of different immunoglobulin isotypes and IgG sub-classes from SIOD patients. These analyses revealed that IgM and IgA levels were normal in all patients and total IgG levels were normal in 70% of patients (Supplemental Table S6). SIOD patients have a selective reduction of IgG_2. The variable concentration of IgG_4 prevented conclusions about IgG_4 levels in SIOD patients. After birth, blood IgG_2 and IgG_4 take approximately 8–10 years longer to reach adult levels than do IgG_1 and IgG_3 [35]. Since most of the patients were very young, the reduced IgG_2 and variable IgG_4 levels might have been age-related.

The deficiency of IL7Rα could arise from either i) mutation(s) of the *IL7R* gene [24,25] or ii) reduced transcription of this gene. To assess the first possibility, we analyzed the coding regions of the *IL7R* gene in SIOD patients; however, we only detected common polymorphisms. To assess the second possibility, we analyzed the expression of *IL7R* mRNA and observed that SIOD T cells had reduced *IL7R* mRNA levels, suggesting that there is reduced transcription of *IL7R*. Hypermethylation of CpG sites in the *IL7R* promoter abolishes the expression of this gene in T cells [23]. To determine whether this could account for the loss of transcription of *IL7R* in SIOD patients, we analyzed the methylation status of the same CpG sites in the *IL7R* promoter of $CD3^+$ T cells obtained from 7 SIOD patients and found hypermethylation of 5 of those 6 CpG sites. We hypothesize that this hypermethylation of the *IL7R* promoter contributes to the reduced expression of *IL7R* and IL7Rα and thereby the T-cell deficiency of SIOD.

We cannot absolutely indict IL7Rα deficiency as the sole cause of T-cell deficiency in SIOD because *SMARCAL1* deficiency, combined with other genetic and environmental factors, alters the expression of

many genes to cause disease [17]. Analysis of the transcriptome, therefore, is necessary to exclude altered expression of other genes involved in T-cell development, especially in the thymic stromal cells. Additionally, global evaluation of genome methylation patterns might provide insights into the role of DNA methylation in causing this and other features of SIOD. The findings of IL7Rα deficiency and methylation of the *IL7R* promoter do, nonetheless, provide one plausible explanation that is consistently observed in each SIOD patient with T-cell immunodeficiency.

In summary, the lack of IL7Rα expression and IL-7 responsiveness in T cells is a hallmark of T-cell immunodeficiency in SIOD and could serve as diagnostic adjuncts (Supplemental Fig. S3). Based on the hypermethylation of the *IL7R* promoter in SIOD T cells and the observations that DNA methyltransferase inhibitors such as 5-azacytidine increase T-cell counts and subsequent survival of patients with high-risk myelodysplastic syndrome [36], we hypothesize that a similar strategy might reactivate transcription of *IL7R* and thereby be a therapy for the T-cell immunodeficiency in SIOD.

Conflict of interest statement

None of the authors has any potential financial conflict of interest related to this manuscript.

Acknowledgments

We would like to thank all of the patients and family members who have contributed to this study. This work was supported in part by grants from the Dana Foundation (C.F.B. and D.B.L.); the Burroughs Wellcome Foundation (1003400) (C.F.B.); the Association Autour D'Emeric et D'Anthony (C.F.B.); the Michael Smith Foundation for Health Research ((CI-SCH-O1899(07-1)) (C.F.B.); the Little Giants Foundation (C.F.B.); the Child & Family Research Institute of British Columbia Children's Hospital (C.F.B.); and the Asociacion Española de Displasias Oseas Minoritarias (C.F.B.). M.M. was supported by a Four Year Doctoral Fellowship from the University of British Columbia. C.F.B. is a scholar of the Michael Smith Foundation for Health Research and a Clinical Investigator of the Child & Family Research Institute. We would like to thank BioServe (Beltsville, MD) for assistance with recruiting age-matched, sex-matched individuals for the unaffected control blood samples.

Appendix A. Supplementary data

Supplementary data to this article can be found online at http://dx.doi.org/10.1016/j.clim.2015.10.005.

References

[1] R.N. Schimke, W.A. Horton, C.R. King, Chondroitin-6-sulphaturia, defective cellular immunity, and nephrotic syndrome, Lancet 2 (1971) 1088–1089.
[2] J. Spranger, G.K. Hinkel, H. Stoss, W. Thoenes, D. Wargowski, F. Zepp, Schimke immuno-osseous dysplasia: a newly recognized multisystem disease, J. Pediatr. 119 (1991) 64–72.
[3] J.H. Ehrich, W. Burchert, E. Schirg, F. Krull, G. Offner, P.F. Hoyer, J. Brodehl, Steroid resistant nephrotic syndrome associated with spondyloepiphyseal dysplasia, transient ischemic attacks and lymphopenia, Clin. Nephrol. 43 (1995) 89–95.
[4] J.M. Saraiva, A. Dinis, C. Resende, E. Faria, C. Gomes, A.J. Correia, J. Gil, N. da Fonseca, Schimke immuno-osseous dysplasia: case report and review of 25 patients, J. Med. Genet. 36 (1999) 786–789.
[5] C.F. Boerkoel, S. O'Neill, J.L. Andre, P.J. Benke, R. Bogdanovic, M. Bulla, A. Burguet, S. Cockfield, I. Cordeiro, J.H. Ehrich, S. Frund, D.F. Geary, A. Ieshima, F. Illies, M.W. Joseph, I. Kaitila, G. Lama, B. Leheup, M.D. Ludman, D.R. McLeod, A. Medeira, D.V. Milford, T. Ormala, Z. Rener-Primec, A. Santava, H.G. Santos, B. Schmidt, G.C. Smith, J. Spranger, N. Zupancic, R. Weksberg, Manifestations and treatment of Schimke immuno-osseous dysplasia: 14 new cases and a review of the literature, Eur. J. Pediatr. 159 (2000) 1–7.
[6] M.A. da Fonseca, Dental findings in the Schimke immuno-osseous dysplasia, Am. J. Med. Genet. 93 (2000) 158–160.
[7] A.S. Dhillon, S. Chapman, D.V. Milford, Cerebellar defect associated with Schimke immuno-osseous dysplasia, Eur. J. Pediatr. 160 (2001) 372–374.
[8] S.S. Kilic, O. Donmez, E.A. Sloan, L.I. Elizondo, C. Huang, J.L. Andre, R. Bogdanovic, S. Cockfield, I. Cordeiro, G. Deschenes, S. Frund, I. Kaitila, G. Lama, P. Lamfers, T. Lucke, D.V. Milford, L. Najera, F. Rodrigo, J.M. Saraiva, B. Schmidt, G.C. Smith, N. Stajic, A. Stein, D. Taha, D. Wand, D. Armstrong, C.F. Boerkoel, Association of migraine-like headaches with Schimke immuno-osseous dysplasia, Am. J. Med. Genet. A 135 (2005) 206–210.
[9] K. Hashimoto, A. Takeuchi, A. Ieshima, M. Takada, M. Kasagi, Juvenile variant of Schimke immunoosseous dysplasia, Am. J. Med. Genet. 49 (1994) 266–269.
[10] G. Lama, N. Marrone, M. Majorana, F. Cirillo, M.E. Salsano, M.M. Rinaldi, Spondyloepiphyseal dysplasia tarda and nephrotic syndrome in three siblings, Pediatr. Nephrol. 9 (1995) 19–23.
[11] C.F. Boerkoel, H. Takashima, J. John, J. Yan, P. Stankiewicz, L. Rosenbarker, J.L. Andre, R. Bogdanovic, A. Burguet, S. Cockfield, I. Cordeiro, S. Frund, F. Illies, M. Joseph, I. Kaitila, G. Lama, C. Loirat, D.R. McLeod, D.V. Milford, E.M. Petty, F. Rodrigo, J.M. Saraiva, B. Schmidt, G.C. Smith, J. Spranger, A. Stein, H. Thiele, J. Tizard, R. Weksberg, J.R. Lupski, D.W. Stockton, Mutant chromatin remodeling protein SMARCAL1 causes Schimke immuno-osseous dysplasia, Nat. Genet. 30 (2002) 215–220.
[12] M.A. Coleman, J.A. Eisen, H.W. Mohrenweiser, Cloning and characterization of HARP/SMARCAL1: a prokaryotic HepA-related SNF2 helicase protein from human and mouse, Genomics 65 (2000) 274–282.
[13] L. Neigeborn, M. Carlson, Genes affecting the regulation of SUC2 gene expression by glucose repression in Saccharomyces cerevisiae, Genetics 108 (1984) 845–858.
[14] M. Stern, R. Jensen, I. Herskowitz, Five SWI genes are required for expression of the HO gene in yeast, J. Mol. Biol. 178 (1984) 853–868.
[15] T. Yusufzai, J.T. Kadonaga, HARP is an ATP-driven annealing helicase, Science 322 (2008) 748–750.
[16] C.E. Bansbach, R. Betous, C.A. Lovejoy, G.G. Glick, D. Cortez, The annealing helicase SMARCAL1 maintains genome integrity at stalled replication forks, Genes Dev. 23 (2009) 2405–2414.
[17] A. Baradaran-Heravi, K.S. Cho, B. Tolhuis, M. Sanyal, O. Morozova, M. Morimoto, L.I. Elizondo, D. Bridgewater, J. Lubieniecka, K. Beirnes, C. Myung, D. Leung, H.K. Fam, K. Choi, Y. Huang, K.Y. Dionis, J. Zonana, K. Keller, P. Stenzel, C. Mayfield, T. Lucke, A. Bokenkamp, M.A. Marra, M. van Lohuizen, D.B. Lewis, C. Shaw, C.F. Boerkoel, Penetrance of biallelic SMARCAL1 mutations is associated with environmental and genetic disturbances of gene expression. Hum. Mol. Genet., 21 (2012) 2572–2587.
[18] A. Baradaran-Heravi, A. Raams, J. Lubieniecka, K.S. Cho, K.A. DeHaai, M. Basiratnia, P.O. Mari, Y. Xue, M. Rauth, A.H. Olney, M. Shago, K. Choi, R.A. Weksberg, M.J. Nowaczyk, W. Wang, N.G. Jaspers, C.F. Boerkoel, SMARCAL1 deficiency predisposes to non-Hodgkin lymphoma and hypersensitivity to genotoxic agents in vivo, Am. J. Med. Genet. A 158A (2012) 2204–2213.
[19] R. Betous, A.C. Mason, R.P. Rambo, C.E. Bansbach, A. Badu-Nkansah, B.M. Sirbu, B.F. Eichman, D. Cortez, SMARCAL1 catalyzes fork regression and Holliday junction migration to maintain genome stability during DNA replication, Genes Dev. 26 (2012) 151–162.
[20] J. Yuan, G. Ghosal, J. Chen, The annealing helicase HARP protects stalled replication forks, Genes Dev. 23 (2009) 2394–2399.
[21] L.I. Elizondo, K.S. Cho, W. Zhang, J. Yan, C. Huang, Y. Huang, K. Choi, E.A. Sloan, K. Deguchi, S. Lou, A. Baradaran-Heravi, H. Takashima, T. Lucke, F.A. Quiocho, C.F. Boerkoel, Schimke immuno-osseous dysplasia: SMARCAL1 loss-of-function and phenotypic correlation, J. Med. Genet. 46 (2009) 49–59.
[22] A.L. Bookout, D.J. Mangelsdorf, Quantitative real-time PCR protocol for analysis of nuclear receptor signaling pathways, Nucl. Recept. Signal. 1 (2003), e012.
[23] H.R. Kim, K.A. Hwang, K.C. Kim, I. Kang, Down-regulation of IL-7Ralpha expression in human T cells via DNA methylation, J. Immunol. 178 (2007) 5473–5479.
[24] A. Puel, S.F. Ziegler, R.H. Buckley, W.J. Leonard, Defective IL7R expression in T(−)B(+)NK(+) severe combined immunodeficiency, Nat. Genet. 20 (1998) 394–397.
[25] C.M. Roifman, J. Zhang, D. Chitayat, N. Sharfe, A partial deficiency of interleukin-7R alpha is sufficient to abrogate T-cell development and cause severe combined immunodeficiency, Blood 96 (2000) 2803–2807.
[26] S. Junge, B. Kloeckener-Gruissem, R. Zufferey, A. Keisker, B. Salgo, J.C. Fauchere, F. Scherer, T. Shalaby, M. Grotzer, U. Siler, R. Seger, T. Gungor, Correlation between recent thymic emigrants and CD31+ (PECAM-1) CD4+ T cells in normal individuals during aging and in lymphopenic children, Eur. J. Immunol. 37 (2007) 3270–3280.
[27] B. Dekel, S. Metsuyanim, N. Goldstein, N. Pode-Shakked, Y. Kovalski, Y. Cohen, M. Davidovits, Y. Anikster, Schimke immuno-osseous dysplasia: expression of SMARCAL1 in blood and kidney provides novel insight into disease phenotype, Pediatr. Res. 63 (2008) 398–403.
[28] F.S. Rosen, M.D. Cooper, R.J. Wedgwood, The primary immunodeficiencies, N. Engl. J. Med. 333 (1995) 431–440.
[29] A. Lev, N. Amariglio, Y. Levy, Z. Spirer, Y. Anikster, G. Rechavi, B. Dekel, R. Somech, Molecular assessment of thymic capacities in patients with Schimke immuno-osseous dysplasia, Clin. Immunol. 133 (2009) 375–381.
[30] M.J. Maeurer, M.T. Lotze, Interleukin-7 (IL-7) knockout mice, implications for lymphopoiesis and organ-specific immunity, Int. Rev. Immunol. 16 (1998) 309–322.
[31] U. von Freeden-Jeffry, P. Vieira, L.A. Lucian, T. McNeil, S.E. Burdach, R. Murray, Lymphopenia in interleukin (IL)-7 gene-deleted mice identifies IL-7 as a nonredundant cytokine, J. Exp. Med. 181 (1995) 1519–1526.
[32] M.J. Palmer, V.S. Mahajan, L.C. Trajman, D.J. Irvine, D.A. Lauffenburger, J. Chen, Interleukin-7 receptor signaling network: an integrated systems perspective, Cell. Mol. Immunol. 5 (2008) 79–89.
[33] J.J. Peschon, P.J. Morrissey, K.H. Grabstein, F.J. Ramsdell, E. Maraskovsky, B.C. Gliniak, L.S. Park, S.F. Ziegler, D.E. Williams, C.B. Ware, J.D. Meyer, B.L. Davison, Early lymphocyte expansion is severely impaired in interleukin 7 receptor-deficient mice, J. Exp. Med. 180 (1994) 1955–1960.

[34] P.P. Zenatti, D. Ribeiro, W. Li, L. Zuurbier, M.C. Silva, M. Paganin, J. Tritapoe, J.A. Hixon, A.B. Silveira, B.A. Cardoso, L.M. Sarmento, N. Correia, M.L. Toribio, J. Kobarg, M. Horstmann, R. Pieters, S.R. Brandalise, A.A. Ferrando, J.P. Meijerink, S.K. Durum, J.A. Yunes, J.T. Barata, Oncogenic IL7R gain-of-function mutations in childhood T-cell acute lymphoblastic leukemia, Nat. Genet. 43 (2011) 932–939.

[35] R.H. Buckley, T Lymphocytes, B Lymphocytes, and Natural Killer Cells (Chapter 123), in: B.M.D.S. Robert, M. Kliegman, J. St. Geme, N.F. Schor, R.E. Behrman (Eds.), Nelson Textbook of Pediatrics, Elsevier Health Sciences 2015, pp. 1006–1012.

[36] P. Fenaux, G.J. Mufti, E. Hellstrom-Lindberg, V. Santini, C. Finelli, A. Giagounidis, R. Schoch, N. Gattermann, G. Sanz, A. List, S.D. Gore, J.F. Seymour, J.M. Bennett, J. Byrd, J. Backstrom, L. Zimmerman, D. McKenzie, C. Beach, L.R. Silverman, M.D.S.S.S.G. International vidaza high-risk, efficacy of azacitidine compared with that of conventional care regimens in the treatment of higher-risk myelodysplastic syndromes: a randomised, open-label, phase III study, Lancet Oncol. 10 (2009) 223–232.

[37] J.M. Clewing, H. Fryssira, D. Goodman, S.F. Smithson, E.A. Sloan, S. Lou, Y. Huang, K. Choi, T. Lucke, H. Alpay, J.L. Andre, Y. Asakura, N. Biebuyck-Gouge, R. Bogdanovic, D. Bonneau, C. Cancrini, P. Cochat, S. Cockfield, L. Collard, I. Cordeiro, V. Cormier-Daire, K. Cransberg, K. Cutka, G. Deschenes, J.H. Ehrich, S. Frund, H. Georgaki, E. Guillen-Navarro, B. Hinkelmann, M. Kanariou, B. Kasap, S.S. Kilic, G. Lama, P. Lamfers, C. Loirat, S. Majore, D. Milford, D. Morin, N. Ozdemir, B.F. Pontz, W. Proesmans, S. Psoni, H. Reichenbach, S. Reif, C. Rusu, J.M. Saraiva, O. Sakallioglu, B. Schmidt, L. Shoemaker, S. Sigaudy, G. Smith, F. Sotsiou, N. Stajic, A. Stein, A. Stray-Pedersen, D. Taha, S. Taque, J. Tizard, M. Tsimaratos, N.A. Wong, C.F. Boerkoel, Schimke immunoosseous dysplasia: suggestions of genetic diversity, Hum. Mutat. 28 (2007) 273–283.

Supplemental data

Title:

Lack of IL7Rα expression in T cells is a hallmark of T-cell immunodeficiency in Schimke immuno-osseous dysplasia (SIOD)

Authors:

Mrinmoy Sanyal[a,b,1,*], Marie Morimoto[c,1], Alireza Baradaran-Heravi[d,1], Kunho Choi[c,1], Neeraja Kambham[b], Kent Jensen[e], Suparna Dutt[e], Kira Y. Dionis-Petersen[f], Lan Xiang Liu[f], Katie Felix[g], Christy Mayfield[h], Benjamin Dekel[i], Arend Bokenkamp[j], Helen Fryssira[k], Encarna Guillen-Navarro[l], Giuliana Lama[m], Milena Brugnara[n], Thomas Lücke[o], Ann Haskins Olney[p], Tracy E. Hunley[q], Ayse Ipek Polat[r], Uluc Yis[r], Radovan Bogdanovic[s], Katarina Mitrovic[s], Susan Berry[t], Lydia Najera[t], Behzad Najafian[u], Mattia Gentile[v], C. Nur Semerci[w], Michel Tsimaratos[x], David B. Lewis[f], and Cornelius F. Boerkoel[c,*]

.Contents

Supplemental Figure Legends

Supplemental Figure S1. Establishment of the IL-7 induced proliferation assay. PBMCs from a normal donor were labeled with CFSE, and cultured for 96 hours. After incubation for 96 hours, T cell subsets were resolved using fluorochrome conjugated anti-human CD3, CD4 and CD8 antibodies. Cellular proliferation was measured by CFSE dilution. (A) Cells were stimulated with increasing concentrations of IL-7 (1-1000 ng/ml). Note that IL-7 alone did not induce proliferation of T cells at any concentration between 1 and 1000 ng/ml either in $CD4^+$ (left column) or $CD8^+$ (right column) cells. (B) Cells were stimulated with anti-CD3/CD28 conjugated beads at a 1:1 or 1:100 bead to cell ratio to induce T-cell proliferation. Note that at a 1:1 bead to cell ratio, the majority of the T cells (both $CD4^+$ or $CD8^+$, upper panels) proliferated. Middle panels show the proliferation of T cells at a 1:100 (sub-optimal) bead to cell ratio and cells showed moderate proliferation. Lower panels show the proliferation of T cells at a 1:100 bead-to-cell ratio in the presence of 10 ng/ml IL-7. Note that addition of IL-7 increased proliferation of T cells (both $CD4^+$ or $CD8^+$) above the values for stimulation with a 1:100 bead to cell ratio alone. Subsequently, we used this assay for IL-7 induced enhancement of proliferation to interrogate the responsiveness SIOD T cells to IL-7 (Figure 4).

Supplemental Figure S2. Effect of IL-2 on the proliferation of SIOD T cells. PBMCs were labeled with CFSE, and cultured for 96 hours. Anti-CD3/CD28 conjugated beads at a 1:100 bead to cell ratio were used to induce T cell proliferation. Cells were incubated with 10 IU/ml IL-2 to determine its effect on T cells with or without anti-CD3/CD28 beads. After incubation for 96 hours, T-cell subsets were resolved using fluorochrome conjugated anti-human CD3, CD4 and CD8 antibodies. Cellular proliferation was measured by CFSE dilution. A representative analysis from one SIOD patient and normal control is shown here. Note that the $CD4^+$ T cells (A) respond to IL-2 induced enhancement of T-cell proliferation. A similar IL-2 response was

observed in SIOD $CD8^+$ T cells (B). SIOD T cells also responded normally to optimum CD3/CD28 bead (1:1 bead to cell ratio) and PHA.

Supplemental Figure S3. FACS analyses for CD3 and IL7Rα expression in the PBMCs of SIOD patients. PBMCs isolated from patient blood were stained with anti-human CD3 and IL7Rα (CD127) antibodies as described in the Methods section. Gated live cells are shown here for the expression of CD3 and IL7Rα. Note that immunodeficient SIOD patients do not express IL7Rα on their T cells.

Supplemental Table S1. Antibodies used for flow cytometry

Antigen	Clone	Conjugation
CD3	UCHT1	Alexa 700
CD4	SK3	Cy7PE
CD8	SK1	Cy7APC
CD45RA	HI100	PE
CD45RO	UCHL1	PerCP5.5
CD25	M-A251	FITC
CD127	HIL-7R-M21	APC
CD19	H1B19	V450
CD25	M-A251	FITC
CD31	WM59	FITC

Supplemental Table S2. Primer sequences for the analysis of *IL7R* gene expression by quantitative PCR

Primer	Sequence
GAPDH-cDNA-F	5'-CTTTTGCGTCGCCAGCCGAG-3'
GAPDH-cDNA-R	5'-GGTGACCAGGCGCCCAATACG-3'
IL7R-cDNA-F	5'-ATGGATCGCAGCACTCACTG-3'
IL7R-cDNA-R	5'-ACGAGGGCCCCACATATTTC-3'

Supplemental Table S3. Primer sequences for the analysis of *SMARCAL1* cDNA mutations by Sanger sequencing

Primer	Sequence
SMARCAL1-cDNA-1F	5'-TGCTTTTGCCAACTTTCCAATTAAA-3'
SMARCAL1-cDNA-1R	5'-TCTTCTGGCTTTTTCCATATTCCC-3'
SMARCAL1-cDNA-2F	5'-AGCCATGGTGTCATTTTCAAGC-3'
SMARCAL1-cDNA-2R	5'-GAGGCTTTTGCTGTCTTGGC-3'
SMARCAL1-cDNA-3F	5'-AACCAAAGAGTTCCCAAGAGACAC-3'
SMARCAL1-cDNA-3R	5'-TGCCATAGGCCCATTCCAGA-3'
SMARCAL1-cDNA-4F	5'-CCTGACACCAAGACGTGGAA-3'
SMARCAL1-cDNA-4R	5'-CAAACGCCAGGGTGAGAGT-3'
SMARCAL1-cDNA-5F	5'-AGCACAGTAAACTAATTGCAAAGGT-3'
SMARCAL1-cDNA-5R	5'-CGACGTTGATGCAATCTGGG-3'
SMARCAL1-cDNA-6F	5'-CAGCCTTTTACCGGAAGGAGT-3'
SMARCAL1-cDNA-6R	5'-GGCATGAAACTGGGGGAAGA-3'
SMARCAL1-cDNA-7F	5'-GGGTGATCCTGTTGTCGGG-3'
SMARCAL1-cDNA-7R	5'-GGGATTTTAGCTTCAGCTGTTCTG-3'
SMARCAL1-cDNA-8F	5'-AACTAAACAGCAGCAGAAAGATGC-3'
SMARCAL1-cDNA-8R	5'-TGGTCTGTCCAATGCGGTG-3'
SMARCAL1-cDNA-9F	5'-GTGTTTGCTGAGCTGTTTTGGAA-3'
SMARCAL1-cDNA-9R	5'-ATCTTCTGCTGCTTTGGGTCC-3'
SMARCAL1-cDNA-10F	5'-CCGGGCTTTCTGAGACCAAT-3'
SMARCAL1-cDNA-10R	5'-CCCTTTTACAGGGGAGACGTAAA-3'

Supplemental Table S4. Primer sequences for the analysis of *IL7R* gene mutations by Sanger sequencing

Primer	Forward primer sequence	Reverse primer sequence
Exon 1	5'-CCTCCCTCCCTTCCTCTTAC-3'	5'-ATTCAAACCCAGTGCCTGAC-3'
Exon 2	5'-TTGGGCTTTTCTTCCTTGAA-3'	5'-AGGAGTTTCAGGAGGCCTTT-3'
Exon 3	5'-ATTCCTGAACATGCCTCCAC-3'	5'-TGCCAGTTGTTTCCACTATTTG-3'
Exon 4	5'-GGTCAAAGTGACTTGCAGAGG-3'	5'-CCCAGGGGAAATGCACTACT-3'
Exon 5	5'-TGGGACTAAAGGAATCCCAAT-3'	5'-CCCTCCAAGGGTGTCCTATT-3'
Exon 6	5'-CAAAGCACCCTGAGACCCTA-3'	5'-GCCTTAATCCCCTTTGTGGT-3'
Exon 7	5'-TGGTCACCCACCTAATTGTG-3'	5'-CCAAAAGGTGAGGTTCAACTG-3'
Exon 8a	5'-ACATGCTGGCAATTCTGTGA-3'	5'-CCTGAGCAACTGGGTTCAAT-3'
Exon 8b	5'-CTGGGAATGTCAGTGCATGT-3'	5'-TCTCTGTGCTGTGAGGGAGA-3'

Supplemental Table S5. Primer sequences for the analysis of *IL7R* promoter methylation by bisulfite pyrosequencing.[23]

CpG Site(s)	Primer	Primer Sequence
-1064	Forward	5'-TGATATATAAATGGGTGAGGTTGT-3'
	Reverse	Biotin-5'-CTTTTTTTTTCCCAAATAAACCTT-3'
	Sequencing	5'-TGATATATAAATGGGTGAGGTTGT-3'
-656	Forward	5'-GTGAAATTTGGAAGTTGGAGGTAA-3'
	Reverse	Biotin-5'-CCCAAATTCAAACAATTCTCCT-3'
	Sequencing	5'-TAGATTTTTTTAAAGTGGGT-3'
-586, -563, -555	Forward	5'-GTGAAATTTGGAAGTTGGAGGTAA-3'
	Reverse	Biotin-5'-CCCAAATTCAAACAATTCTCCT-3'
	Sequencing	5'-AGGTAGATTATTTGAGGTTA-3'
-435	Forward	5'-TTGGGAGGTGAAAATTGTAGTGAG-3'
	Reverse	Biotin-5'-TAAATATTCCCTACAACCCCCACA-3'
	Sequencing	5'-GGAGGTGAAAATTGTAGTG-3'

Supplemental Table S6. Serum immunoglobulin levels in SIOD patients

Patient ID	IgM 19/20	IgG 14/21	IgG_1 16/21	IgG_2 5/22	IgG_3 19/21	IgG_4 9/22	IgA 20/20
SD9	nl	nl	ND	lo	ND	lo	nl
SD18c	nl	nl	nl	lo	nl	lo	nl
SD22	nl	nl	nl	lo	nl	nl	nl
SD24	nl	lo	nl	lo	nl	nl	nl
SD25	nl	lo	lo	lo	nl	nl	nl
SD27	hi	lo	lo	lo	nl	lo	nl
SD38	ND	ND	nl	lo	nl	nl	ND
SD41	nl	nl	nl	nl	nl	nl	nl
SD44	nl	nl	nl	lo	nl	nl	nl
SD47	nl	nl	nl	nl	nl	nl	nl
SD60	nl	nl	nl	lo	nl	lo	nl
SD74	hi	nl	nl	lo	nl	nl	nl
SD94b	nl	lo	nl	lo	nl	lo	lo
SD107	nl	lo	nl	lo	nl	lo	lo
SD108	nl	nl	nl	nl	nl	lo	nl
SD108a	nl	lo	lo	lo	nl	nl	nl
SD108b	nl	nl	nl	nl	nl	nl	nl
SD109	nl	nl	nl	lo	nl	nl	nl
SD114	-	hi	hi	nl	hi	nl	ND
SD136a	nl	nl	lo	lo	lo	nl	nl
SD136b	nl	nl	nl	lo	nl	lo	nl
SD138	nl	lo	lo	lo	lo	lo	nl

nl, normal; lo lower than normal values; hi higher than normal values; ND Not done; numbers below immunoglobulin isotypes and subtypes indicate the number of patients that have a normal level of the indicated immunoglobulin isotype/subtype out of the total number of patients analyzed.

Figure S1

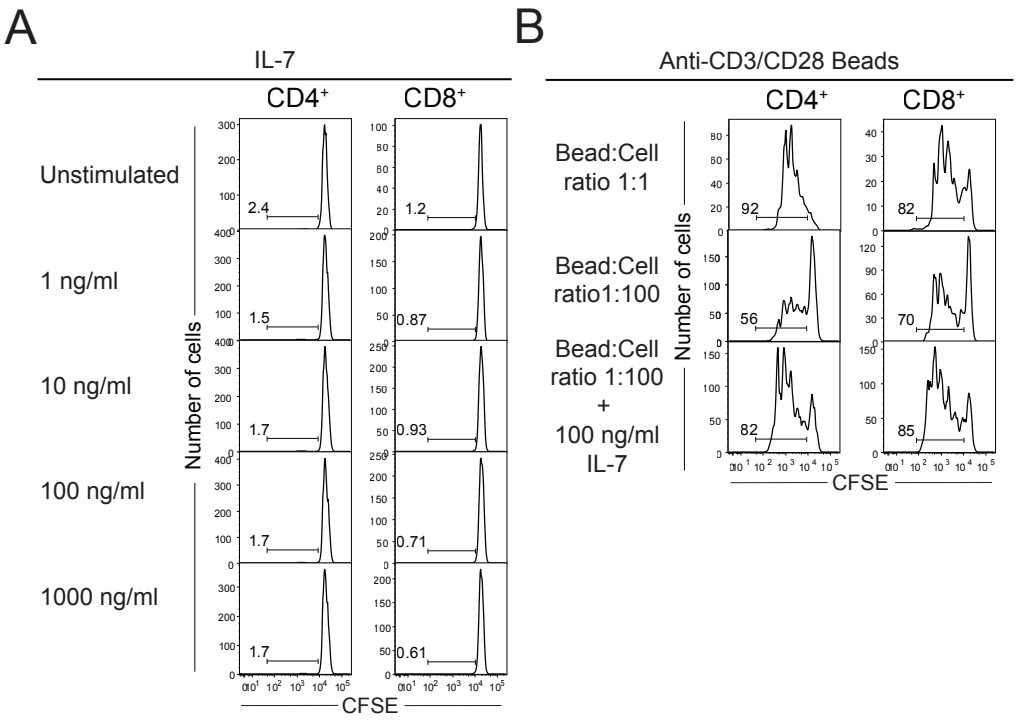
A
IL-7
CD4+
CD8+
Unstimulated
1 ng/ml
10 ng/ml
100 ng/ml
1000 ng/ml
2.4
1.2
1.5
0.87
1.7
0.93
1.7
0.71
1.7
0.61
Number of cells
CFSE
B
Anti-CD3/CD28 Beads
CD4+
CD8+
Bead:Cell ratio 1:1
Bead:Cell ratio1:100
Bead:Cell ratio 1:100 + 100 ng/ml IL-7
92
82
56
70
82
85
Number of cells
CFSE

Figure S2

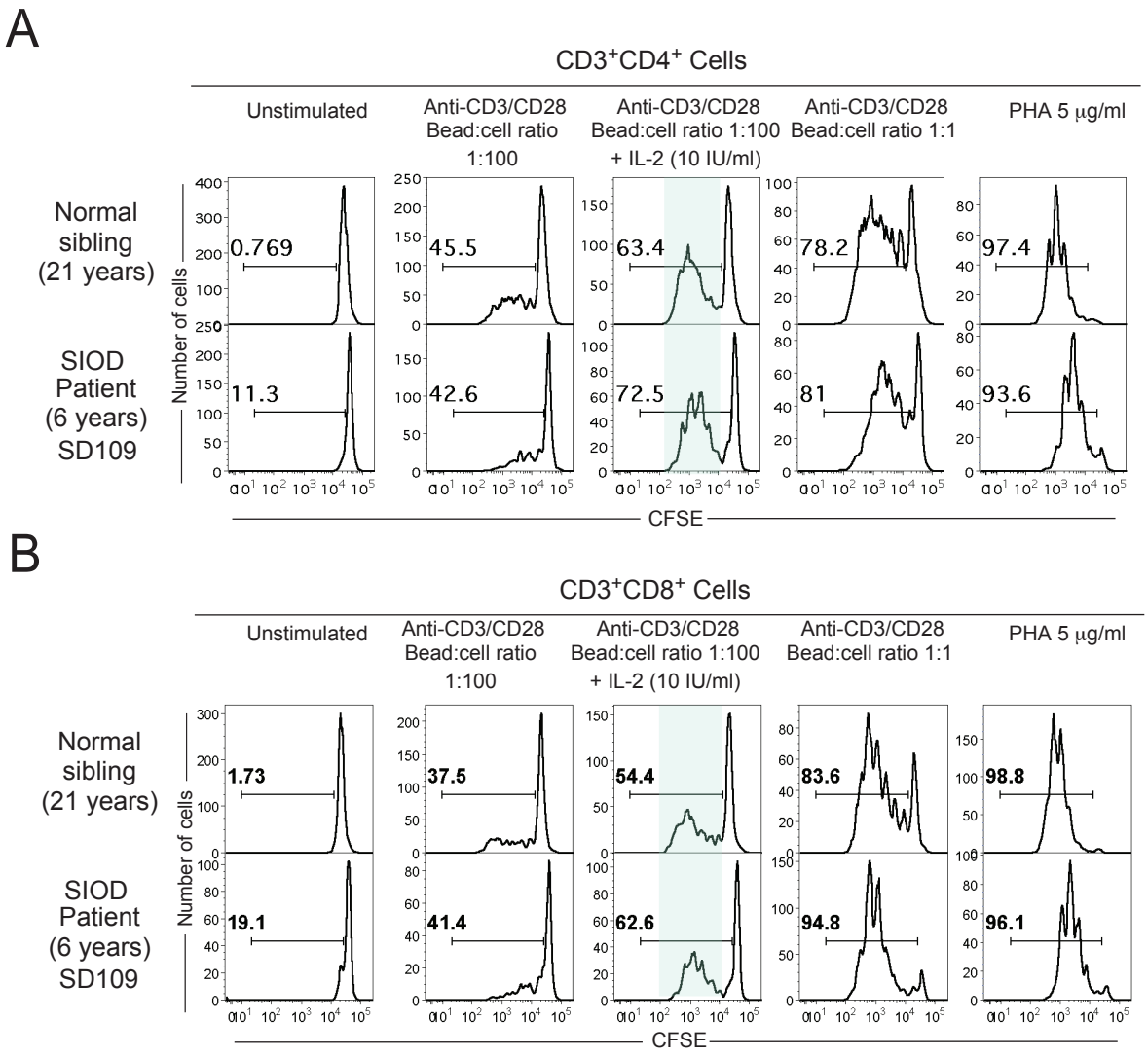
A
CD3+CD4+ Cells
Unstimulated
Anti-CD3/CD28 Bead:cell ratio 1:100
Anti-CD3/CD28 Bead:cell ratio 1:100 + IL-2 (10 IU/ml)
Anti-CD3/CD28 Bead:cell ratio 1:1
PHA 5 μg/ml
Normal sibling (21 years)
SIOD Patient (6 years) SD109
Number of cells
0.769
45.5
63.4
78.2
97.4
11.3
42.6
72.5
81
93.6
CFSE
B
CD3+CD8+ Cells
Unstimulated
Anti-CD3/CD28 Bead:cell ratio 1:100
Anti-CD3/CD28 Bead:cell ratio 1:100 + IL-2 (10 IU/ml)
Anti-CD3/CD28 Bead:cell ratio 1:1
PHA 5 μg/ml
Normal sibling (21 years)
SIOD Patient (6 years) SD109
Number of cells
1.73
37.5
54.4
83.6
98.8
19.1
41.4
62.6
94.8
96.1
CFSE

Figure S3

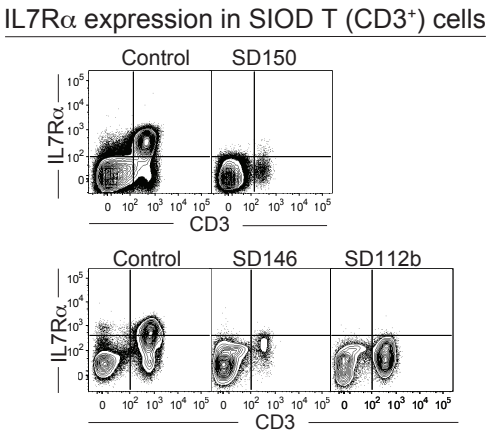
IL7Rα expression in SIOD T (CD3+) cells
Control
SD150
IL7Rα
CD3
Control
SD146
SD112b
IL7Rα
CD3